Polymer Chemistry

Synthesis of Bottlebrush Polymers Based on Poly(*N*-Sulfonyl Aziridine) Macromonomers

Journal:	*Polymer Chemistry*
Manuscript ID	PY-ART-08-2022-001125.R1
Article Type:	Paper
Date Submitted by the Author:	30-Sep-2022
Complete List of Authors:	Archer, William; Virginia Tech, Chemistry Dinges, Grace; Virginia Tech, Chemistry MacNicol, Piper; Virginia Tech, Chemistry Schulz, Michael; Virginia Tech, Chemistry

Synthesis of Bottlebrush Polymers Based on Poly(*N*-Sulfonyl Aziridine) Macromonomers

William R. Archer[1], Grace E. Dinges[1], Piper L. MacNicol[1], and Michael D. Schulz[1]*

1: Department of Chemistry and Macromolecules Innovation Institute

Virginia Tech, Blacksburg, VA USA 24061

* Correspondence to mdschulz@vt.edu

(GED and PLM contributed equally to this work)

Abstract

We synthesized bottlebrush polymers with polyaziridine brushes and a polynorbornene backbone by a grafting-through approach. Polyaziridine macromonomers were synthesized by aza-anoinic polymerization of an *N*-tosylaziridine, initiated with a norbornene-functionalized sulfonamide anion. These macromonomers were then polymerized by ring-opening metathesis polymerization (ROMP) in dichloromethane to produce bottlebrush polymers with molecular weights of 136–456 kDa. To investigate potential macromonomer aggregation that would hinder grafting-through polymerization, we used dynamic light scattering (DLS) to measure the change in macromonomer aggregation and the growth of bottlebrush chains during ROMP. We observed that the macromonomers aggregate in solution, but once ROMP is initiated, these aggregates disperse over the course of the polymerization. This solution behavior appears to be an example of polymerization-induced deaggregation.

Introduction

The unique properties of bottlebrush polymers are well documented in the literature and often derive from both the structure of the sidechain and the topology of the bottlebrush polymer itself.[1-5] At high degrees of polymerization, bottlebrush polymers demonstrate a sphere-to-cylinder transition resulting from the stretching of the polymer backbone[6], and as a result of their unique topology, have found many applications as lubricants, nanostructured coatings, and photonic crystals.[7-10] While several synthetic approaches can lead to bottlebrush polymers, the grafting-through method is particularly useful as it produces "perfectly" grafted materials.[11-14] This approach relies on first synthesizing macromonomers (MM)—polymers with a polymerizable end-group—which are subsequently polymerized to give the final bottlebrush topology. Ring-opening metathesis polymerization (ROMP) has proven particularly effective in grafting-through polymerization due to the high activity and functional group tolerance of well-defined olefin metathesis catalysts.[15-17] Thus, ROMP is commonly used in conjunction with other polymerization methods (e.g., atom transfer radical polymerization[18], ring-opening polymerization[19], and cross-coupling polymerizations[20]) to produce bottlebrush polymers.

Aza-anionic ring-opening polymerization of *N*-tosylaziridines has proven to be a reliable method to produce linear polyaziridines.[21, 22] These polymerizations rely on the electron-withdrawing ability of a sulfonyl group, which facilitates nucleophilic attack of the aziridine ring.[23] As a result, polymerization of *N*-tosylaziridines has been used in thermosetting materials,[24] block copolymers,[25-27] and post-polymerization modifications.[28] Furthermore, the resulting poly(*N*-tosylaziridines) can be reduced to produce linear polyamines for water purification, non-viral gene delivery, and further post-polymerization

modifications.[29-34] However, aza-anionic polymerizations have largely been limited to synthesizing linear polymers. Building on these developments, we synthesized a series of bottlebrush polyaziridines from a norbornene-functionalized poly(*N*-tosylaziridine) MM prepared by aza-anionic polymerization of an activated aziridine monomer, followed by ROMP of the norbornene end-group.

Experimental

Materials

4-Toluenesulfonyl chloride (TsCl), methanesulfonyl chloride (MsCl), potassium bis(trimethylsilyl) amide (KHMDS), and 2-aminopropanol were purchased from Sigma Aldrich. Pyridine, potassium hydroxide, and *N*-Boc-ethylenediamine were obtained from Oakwood Chemical. Exo-norbornene anhydride was synthesized accordingly to a previously reported procedure and recrystallized from benzene prior to use.[35] Toluene, dichloromethane (DCM), and diethylether were purchased from Fisher Scientific. All chemicals were used as-is, unless otherwise stated.

Measurements

^{1}H and ^{13}C NMR data were collected at 25 ºC using an Agilent U4-DD2 400 MHz spectrometer. Chemical shifts in the ^{1}H NMR and ^{13}C NMR spectra were referenced to the residual solvent resonance signals.

Molecular weight analysis of the macromonomer was conducted using an ACQUITY Advanced Polymer Chromatography (APC) system consisting of Omnisec light scattering and refractive index detectors, and ACQUITY APC XT 2.5 μm columns heated to 40 ºC with a dimethylformamide (DMF) mobile phase. Data analysis was performed

using the OMNISEC software version 11.10 (Malvern Panalytical). The molecular weight of the macromonomer was calculated using traditional calibration with 5 polymethyl methacrylate standards (M_p = 1,810–146,500 g mol^{-1}).

Size-exclusion chromatography (SEC) of the bottlebrush polymers was performed using Wyatt Technologies TRIOS II light scattering and Optilab T-REX refractive index detectors. Two Agilent Technologies PLgel 10 μm mixed-bed columns heated to 50 ºC were used with a mobile phase consisting of *N*,*N*-dimethylacetamide (DMAc) with 50 mM lithium chloride as the eluent and a Shimadzu LC-20AD with pump operating at 1.0 mL min^{-1}. Data analysis was performed using Astra version 7.2.2.10 software (Wyatt Technologies). The dn/dc of the bottlebrush polymers were measured offline in DMAc with the Optilab T-REX differential refractometer using a series of bottlebrush polymer solutions of concentrations 1–5 mg mL^{-1}. The MM is not soluble in DMAc, thus residual MM from the grafting-through polymerization was removed by filtration prior to molecular weight analysis.

Dynamic light scattering was conducted using a Malvern Instruments (Worchestershire, UK) Zetasizer Nano-ZS. Samples were filtered using .22 μm filters before analysis. Following a 2-minute equilibration, samples were recorded for 120 seconds, and three accumulated runs were averaged to obtain the particle size distribution. The raw correlation functions for these DLS experiments are included in the ESI (**Fig. S12**).

Synthesis of 2-methyl-1-tosylazirdine monomer

2-Methylaziridine was synthesized in a two-step reaction according to a modified procedure previously reported for tosylaziridine.[36] In the first step, TsCl (29.08 g, 152 mmol, 2.2 eqiv.) was dissolved in pyridine (200 mL) in a salt–ice bath and allowed to stir

for 20 min. 2-Aminopropanol (5.2 g, 69 mmol, 1.0 equiv.) was dissolved in 10 mL of pyridine and added dropwise to the stirred solution. Following the complete addition of 2-aminopropanol, the reaction was allowed to warm to room temperature and stirred for 15 h. DI water (100 mL) was added to dissolve the solid. The reaction mixture was extracted with DCM (150 mL × 3) and washed with 3 M HCl (100 mL × 3). The organic layers were dried over $MgSO_4$ and concentrated. The resulting oil was purified using flash column chromatography (80:20, hexanes:acetone, $R_f = 0.142$) to provide a yellow–orange oil in 85% yield.

In the second step, the ditosylated product from step 1 (12.62 g, 32.9 mmol, 1.0 equiv.) was dissolved in 150 mL of toluene in an Erlenmeyer flask. KOH (6.4 g, 115.4 mmol, 3.5 equiv.) was dissolved in 30 mL of DI water. The KOH solution was added dropwise to the Erlenmeyer flask and allowed to stir at 22 ºC for 1 h. 100 mL of H_2O was added and the reaction was extracted with diethyl ether (50 mL × 3). The combined organic layers were washed with $NaHCO_3$ (20 mL × 2), dried with $MgSO_4$, and concentrated *in vacuo* to afford the tosylated 2-methyl aziridine monomer as a white solid (70 % yield). ^1H and ^{13}C NMR of the purified product matched previously reported literature spectra.[37] ^1H NMR (400 MHz, $CDCl_3$, δ): 1.26 (d, 3H), 1.55 (s, 1H), 2.02 (d, 1 H), 2.45 (d, 3H), 2.62 (d, 1H), 2.83 (m, 1H), 7.34 (m, 2H), 7.82 (m, 2H). ^{13}C NMR (100 MHz, $CDCl_3$, δ): 16.7, 21.6, 34.7, 35.8, 127.8, 129.7, 144.4 (**Figs. S3 and S4**).

Synthesis of Norbornene Aza-anionic Initiator (Nor–MS)

The aza-anionic norbornene initiator (Nor–Ms) was synthesized via a two-step reaction. In the first step, exo-norbornene anhydride (1.9 g, 12.0 mmol, 1.0 equiv) was combined in toluene with *N*-Boc-ethylenediamine (2.1 g, 13.6 mmol, 1.1 equiv). The

reaction mixture was heated to 130 ºC with a Dean-Stark apparatus and condenser for 10 h. After cooling to 22 ºC, the solvent was removed under reduced pressure and the target compound was purified by recrystallization from MeOH to afford a white solid (2.1 g, 57% yield).[38]

To install the mesylate group, the product from the previous step (1.0 g, 3.35 mmol, 1.0 equiv) was first dissolved in 3 mL DCM with 3 mL of HCl (*aq*) to remove the Boc protecting group. After stirring for 30 min, the reaction was placed in an ice bath. NEt_3 (4 equiv) was added dropwise to the stirred solution and allowed to stir for 30 min. MsCl (0.44 g, 3.8 mmol, 1.1 equiv) was added dropwise over 20 min. The reaction was allowed to warm to room temperature and stirred overnight. The resulting solution was washed with 3 M HCl (50 mL × 3), $NaHCO_3$, brine (100 mL × 3), dried with $MgSO_4$, and concentrated, resulting in a white solid (35% yield). ^{1}H NMR (400 MHz, $CDCl_3$, δ): 1.27 (dq,1H), 1.52 (dq, 1H), 2.72 (d, 2H), 2.92 (s, 3 H), 3.26 (m, 2H), 3.34 (m, 2H), 3.67 (m, 2H), 4.81 (t, 1H), 6.27 (m, 2H). ^{13}C NMR (100 MHz, $CDCl_3$, δ): 38.2, 40.6, 41.3, 42.9, 45.1, 47.9, 138.8, 178.3 (**Figs. S6 and S7**).

Synthesis of Poly(2-methyl-1-tosylaziridine) Macromonomer

Nor–Ms (190.0 mg, 0.668 mmol, 1.0 equiv), and KHMDS (134.4 mg, 0.673 mmol, 1.0 equiv) were dissolved in 3 mL of DMF and allowed to stir for 10 min. 2-Methyltosylaziridine (2.34 g, 11.3 mmol, 17 equiv) was dissolved in 8 mL of DMF and heated to 50 ºC in a scintillation vial. After the monomer dissolved, the Nor–Ms mixture was added to the monomer solution in one portion, and stirred for 15 h to ensure complete monomer conversion. The polymerization was terminated by adding a few drops of acidic MeOH. The polymer product was collected by precipitation into cold MeOH, and dried *in*

vaccuo to a constant weight. ($M_n^{(NMR)}$: 4,930 kDa, $M_n^{(SEC)}$: 4,200 kDa, Đ: 1.07) (**Figs. S8 and S9**).

Synthesis of Bottlebrush Polymers with Poly(aziridine) Sidechains

Grubbs third-generation catalyst (G3) was synthesized accordingly to a previously reported procedure and used within 2 days.[39, 40] To synthesize the bottlebrush polymers, a scintillation vial was charged with appropriate amounts of MM and DCM. In addition, trifluoracetic acid (2 equiv. with respect to G3) was added to scavenge any excess pyridine, which would adversely affect the rate of polymerization.[11] To initiate the polymerization, G3 was added in one potion. The polymerization continued to stir for 35 min, after which time the reaction was terminated with the addition of a few drops of ethyl vinyl ether. The bottlebrush polymer was collected by precipitation into diethyl ether, followed by centrifugation (**Fig. S11**). Typical yields of the bottlebrush polymers were 35–70%.

Results and Discussion

Numerous literature reports describe synthetic routes to substituted aziridines.[41] While synthesizing aziridines from the corresponding epoxide,[42] α-amino acid,[43] or olefin[44] has been reported, most commonly vicinal amino alcohol derivatives are transformed to the corresponding aziridine *via* a Wenker aziridine synthesis.[45] Following this approach, we synthesized a tosylated 2-methylaziridine monomer by reacting aminopropanol with tosylchloride, which provided ditosylated 2-aminopropanol. The tosylated aziridine is then easily accessible by reacting the ditosylated product with KOH(aq) in toluene, which

provides the target monomer, 2-methyl-1-tosylaziridine, as a crystalline white solid in good yield (**Fig. 1A**).

Sulfonamide anions, which can be generated by deprotonation of a sulfonamide with potassium hexamethyldisilazide (KHMDS), efficiently initiate aza-anionic polymerizations of activated aziridine monomers.[22, 37, 46] This polymerization places the sulfonamide initiator on the α-end-group of the polymer chain. Here, we used a norbornene containing a methanesulfonamide (MS) group as the initiator, which enabled the synthesis of polymers with a terminal, polymerizable norbornene (**Fig. 1B**). Because the propagating sulfonamide anion is weakly nucleophilic, the aza-anionic polymerization achieves high monomer conversions without side-reactions (e.g., reaction with the norbornene),[23] resulting in completely linear polymers with high end-group fidelity. ^{1}H NMR end-group analysis confirmed successful polymerization: The broad peaks between 7.6–7.9 and 7.1–7.3 ppm correspond to the aromatic tosylate protons in the MM backbone, which indicated an average degree of polymerization (DP) of 22 when compared to the norbornene olefin signal at 6.2 ppm. End-group analysis by NMR indicated an M_n of 4,930 g mol^{-1}, and SEC analysis indicated an M_n 4,200 g mol^{-1} ($M_n^{(Theor)}$: 4,721 g mol^{-1}, Đ: 1.07) (**Fig. S9**).

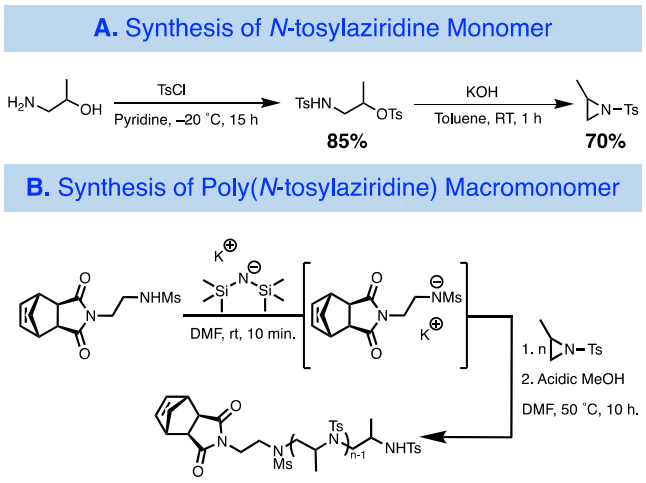

Figure 1. Synthesis of **A.** 2-methyl-1-tosylaziridine monomer and **B.** poly(2-methyl-1-tosylaziridine) macromonomer.

We used this macromonomer to synthesize bottlebrush polymers *via* grafting-through ROMP initiated by Grubbs' third-generation catalyst (G3), which polymerized the MM norbornene chain-end (**Fig. 2A**). We first investigated the grafting-through ROMP kinetics ([MM]:[G3]=100:1) using ^{1}H NMR. Because the tosylate group in the MM backbone is unchanged during ROMP, we monitored the reduction in the norbornene peak relative to the tosylate signals to determine the macromonomer conversion. These experiments revealed pseudo first-order kinetics with respect to the [MM], and the polymerization achieved approximately 70% conversion in 30 min after which time the MM conversion plateaued (**Fig. S10**). This observation is consistent with previously reported kinetics for bottlebrush polymers synthesized by ROMP of a norbornene imide.[11] The low conversion achieved with this MM (particularly when targeting higher DPs, as discussed below) could be due to several factors. For example, the MM contains an amine in every repeat unit that could limit the lifetime of the catalyst and activity, thus preventing higher conversions.[47-49]

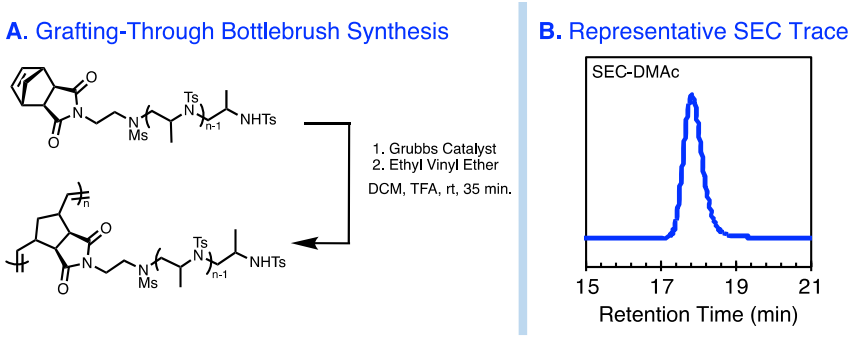

Figure 2. A. Grafting-through synthesis of bottlebrush poly(2-methyl-1-tosylaziridine)s and **B.** representative SEC trace (Table 1, Entry 1) of resulting bottlebrush polymer.

To probe the conversion limitations with this macromonomer, we performed additional bottlebrush polymerizations in which we targeted higher DPs (**Table 1**, Entries 2–5). Following polymerization, we observed a reduction of the peak corresponding to the norbornene olefin in the ^{1}H NMR, and the evolution of signals corresponding to the polynorbornene backbone (**Fig. S11**). We achieved higher MM conversions (~70 %) when targeting bottlebrush polymer DPs less than 300, while we achieved only ~60% conversion in 35 min when targeting DPs of 400 and 500. Entries 1–3 indicate that this MM may exhibit a conversion limit around 70 % in 35 min. However, MM conversion decreased rapidly with increasing [MM]:[G3], suggesting that the bottlebrush polymer is limited to a DP ~100 MM units. This observed ceiling in DP is in agreement with previously reported synthesis of bottlebrush polymers containing a norbornene imide.[11] End-group analysis of these materials was challenging because the benzylidene end-group overlapped with the signals from the tosylate functional groups on the sidechains. Nevertheless, SEC of these materials revealed bottlebrush molecular weights between 136–450 kDa and $Đ < 1.5$ (**Fig. 2B**). The Đ of these bottlebrush polymers is higher than many previously reported bottlebrush polymers, which we believe is due to MM aggregation in dichloromethane (see

light scattering experiments discussed below). The insolubility of the MM in other common ROMP solvents (e.g., EtOAc and *i*-PrOAc) hindered efforts to surmount this issue.[50]

Table 1. Characterization of bottlebrush polymers. [a]Determined by the ^{1}H NMR. [b]Determined by [MM]:[G3] and % Conv. [c]Molecular weight determined from size exclusion chromatography (DMAc, dn/dc determined offline in DMAc).

Entry	[MM]:[G3]	% Conv[a]	$M_n^{(Theor)b}$ (kg mol^{-1})	$M_n^{(SEC)c}$ (kg mol^{-1})	Đ[c]
1	100:1	72	430	136.2	1.26
2	200:1	71	860	303.8	1.28
3	300:1	70	1,200	408.6	1.34
4	400:1	61	1,400	425.0	1.37
5	500:1	59	1,700	456.5	1.40

We used dynamic light scattering (DLS) to investigate MM aggregation in this polymerization (**Fig. 3**). Initially, the MM exists as large aggerates that are approximately 955 nm in diameter. Early in the polymerization after the addition of G3, DLS indicates the formation of unimolecular polymer chains (4 nm), which we believe correspond to the initiated bottlebrush polymer. At 10 minutes, the large aggregates are almost completely gone, while a single species approximately 12 nm in diameter remains. This species continues to grow to 16 nm at 50 min, at which time the polymerization was terminated. The raw correlation functions for these DLS experiments are included in the Supporting Information (**Fig. S12**).

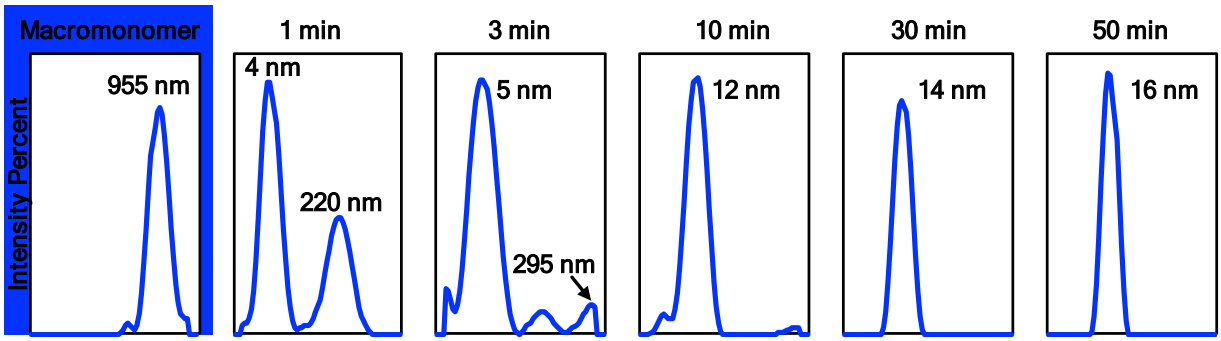

Figure 3. DLS intensity percent during ROMP. Initially, the MM forms large aggregates, however once ROMP is initiated, the MM aggregate size decreases, and the evolution of growing bottlebrush polymer chains is observed.

This (de)aggregation behavior is unusual, as polymerization typically reduces solubility or promotes aggregation.[51-53] In this case, however, we observed polymerization-induced deaggregation. We hypothesize that this deaggregation is driven by changes in the conformation of the polyaziridine brushes caused by polymerization of the end-group. Because the bottlebrush topology enforces an extended-chain conformation, polymerization both forces the polyaziridine chains into an elongated conformation and orients the ω-chain-ends toward the solvent. These changes promote solubilization of the growing bottlebrushes and disperse the aggregates of the macromonomers. While polymer topology is known to strongly influence solubility properties in a variety of materials,[54-57] to the best of our knowledge these experiments are the first example demonstrating the evolution of such a solubility change over the course of a macromonomer polymerization.

Conclusions

In summary, we demonstrated the controlled synthesis of a polyaziridine MM *via* the aza-anionic ring-opening polymerization of an activated aziridine. The high efficiency of the aza-anionic polymerization enabled precise control over the MM molecular weight and dispersity ($M_n^{(SEC)}$: 4,200 g mol^{-1}, Đ: 1.07). The subsequent grafting-through polymerization of the polyaziridine MM achieved between 60–70% conversion in 35 minutes and resulted in bottlebrush polymers that exhibited controlled molecular weights. Finally, we observed an unusual deaggregation behavior during ROMP using DLS in which aggregates of MM were converted to fully dispersed bottlebrush polymers over time. Overall, this study sheds light on the synthesis of novel amine-containing bottlebrush polymers that can guide the future design of functional materials with this unique polymer topology.

Author Contributions

WRA, GED, and PLM synthesized and characterized the materials. WRA and MDS wrote the manuscript. GED and PLM contributed equally.

Conflicts of interest

There are no conflicts to declare.

Acknowledgements

The authors wish to acknowledge the Virginia Tech Department of Chemistry Faculty Start-up funds for financial support. This work was made possible by the use of

Virginia Tech's Materials Characterization Facility, which is supported by the Institute for Critical Technology and Applied Science, the Macromolecules Innovation Institute, and the Office of the Vice President for Research and Innovation. A portion of this work was performed at the Nanoscale Characterization and Fabrication Laboratory, which is supported by the Virginia Tech National Center for Earth and Environmental Nanotechnology Infrastructure (NanoEarth), a member of the National Nanotechnology Coordinated Infrastructure (NNCI), supported by NSF (ECCS 1542100 and ECCS 2025151). This work was also supported by GlycoMIP, a National Science Foundation Materials Innovation Platform funded through Cooperative Agreement DMR-1933525.

References

1. R. Verduzco, X. Li, S. Pesek and G. Stein, *Chem. Soc. Rev.* , 2015, **44**, 2405.
2. Y. Yu, C. Chae, M. Kim, H. Seo, R. Grubbs and J. Lee, *Macromolecules*, 2018, **51**, 447–455.
3. A. B. Chang, T.-P. Lin, N. B. Thompson, S.-X. Luo, A. L. Liberman-Martin, H.-Y. Chen, B. Lee and R. H. Grubbs, *J. Am Chem. Soc.*, 2017, **139**, 17683–17693.
4. X. Li, S. L. Prukop, S. L. Biswal and R. Verduzco, *Macromolecules*, 2012, **45**, 7118–7127.
5. M. Müllner, *Chem. Commun.*, 2022, **58**, 5683-5716.
6. S. L. Pesek, X. Li, B. Hammouda, K. Hong and R. Verduzco, *Macromolecules*, 2013, **46**, 6998–7005.
7. B. M. Boyle, J. L. Collins, T. E. Mensch, M. D. Ryan, B. S. Newell and G. M. Miyake, *Polym. Chem.*, 2020, **11**, 7147–7158.
8. Y. Wu, L. Zhang, M. Zhang, Z. Liu, W. Zhu and K. Zhang, *Polym. Chem.*, 2018, **9**, 1799–1806.
9. M. L. Ohnsorg, P. C. Prendergast, L. L. Robinson, M. R. Bockman, F. S. Bates and T. M. Reineke, *ACS Macro Lett.*, 2021, **10**, 375–381.
10. A. L. Liberman-Martin, C. K. Chu and R. H. Grubbs, *Macromol. Rapid Commun.*, 2017, **38**, 1700058.
11. S. C. Radzinski, J. C. Foster, R. C. Chapleski, D. Troya and J. B. Matson, *J. Am. Chem. Soc.*, 2016, **138**, 6998–7004.
12. S. C. Radzinski, J. C. Foster, S. E. Lewis, E. V. French and J. B. Matson, *Polym. Chem.*, 2017, **8**, 1636–1643.
13. W. J. Wolf, T.-P. Lin and R. H. Grubbs, *J. Am. Chem. Soc.*, 2019, **141**, 17796–17808.

14. T. G. Floyd, S. Häkkinen, S. C. L. Hall, R. M. Dalgliesh, A.-C. Lehnen, M. Hartlieb and S. Perrier, *Macromolecules*, 2021, **54**, 9461–9473.
15. M. Yasir, P. Liu, I. K. Tennie and A. F. M. Kilbinger, *Nat. Chem.*, 2019, **11**, 488–494.
16. J. C. Lee, K. A. Parker and N. S. Sampson, *J. Am. Chem. Soc.*, 2006, **128**, 4578–4579.
17. J. A. Johnson, Y. Y. Lu, A. O. Burts, Y.-H. Lim, M. G. Finn, J. T. Koberstein, N. J. Turro, D. A. Tirrell and R. H. Grubbs, *J. Am. Chem. Soc.*, 2011, **133**, 559–566.
18. W. J. Neary, B. A. Fultz and J. G. Kennemur, *ACS Macro Lett.*, 2018, **7**, 1080–1086.
19. B. B. Patel, D. J. Walsh, D. H. Kim, J. Kwok, B. Lee, D. Guironnet and Y. Diao, *Science Advances*, 2020, **6**, eaaz7202.
20. S.-k. Ahn, D. L. Pickel, W. M. Kochemba, J. Chen, D. Uhrig, J. P. Hinestrosa, J.-M. Carrillo, M. Shao, C. Do, J. M. Messman, W. M. Brown, B. G. Sumpter and S. M. Kilbey, *ACS Macro Lett.*, 2013, **2**, 761–765.
21. T. Gleede, L. Reisman, E. Rieger, P. C. Mbarushimana, P. A. Rupar and F. R. Wurm, *Polym. Chem.*, 2019, **10**, 3257–3283.
22. E. Rieger, T. Gleede, K. Weber, A. Manhart, M. Wagner and F. R. Wurm, *Polym. Chem.*, 2017, **8**, 2824–2832.
23. T. Gleede, E. Rieger, L. Liu, C. Bakkali-Hassani, M. Wagner, S. Carlotti, D. Taton, D. Andrienko and F. R. Wurm, *Macromolecules*, 2018, **51**, 5713–5719.
24. S. Jung, S. Kang, J. Kuwabara and H. J. Yoon, *Polym. Chem.*, 2019, **10**, 4506–4512.
25. H. Huang, W. Luo, L. Zhu, Y. Wang and Z. Zhang, *Polym. Chem.*, 2021, **12**, 5328–5335.
26. T. Gleede, J. C. Markwart, N. Huber, E. Rieger and F. R. Wurm, *Macromolecules*, 2019, **52**, 9703–9714.
27. T. Gleede, E. Rieger, J. Blankenburg, K. Klein and F. R. Wurm, *J. Am Chem. Soc.*, 2018, **140**, 13407–13412.
28. Z. Li, R. Chen, Y. Wang, L. Zhu, W. Luo, Z. Zhang and N. Hadjichristidis, *Polym. Chem.*, 2021, **12**, 1787–1796.
29. T. Gleede, F. Yu, Y.-L. Luo, Y. Yuan, J. Wang and F. R. Wurm, *ACS Macro Lett.*, 2020, **9**, 20–25.
30. L. Reisman, C. P. Mbarushimana, S. J. Cassidy and P. A. Rupar, *ACS Macro Lett.*, 2016, **5**, 1137–1140.
31. P. C. Mbarushimana, Q. Liang, J. M. Allred and P. A. Rupar, *Macromolecules*, 2018, **51**, 977–983.
32. W. R. Archer, B. A. Hall, T. N. Thompson, O. J. Wadsworth and M. D. Schulz, *Polym. Int.* , 2019, **68**, 1220–1237.
33. W. R. Archer, A. Fiorito, S. L. Heinz-Kunert, P. L. MacNicol, S. A. Winn and M. D. Schulz, *Macromolecules*, 2020, **53**, 2061–2068.
34. F. Alexis, S.-L. Lo and S. Wang, *Adv. Mater.* , 2006, **18**, 2174–2178.
35. C. Bates, A. Chang, N. Momc ilovic˘, S. Jones and R. Grubbs, *Macromolecules*, 2015, **48**, 4967–4974.
36. F. Beltran, I. Fabre, I. Ciofini and L. Miesch, *Org. Lett.*, 2017, **19**, 5042–5045.
37. I. C. Stewart, C. C. Lee, R. G. Bergman and F. D. Toste, *J. Am Chem. Soc.*, 2005, **127**, 17616–17617.
38. R. N. Robson and F. M. Pfeffer, *Chem. Commun.*, 2016, **52**, 8719–8721.
39. S. C. Radzinski, J. C. Foster, S. J. Scannelli, J. R. Weaver, K. J. Arrington and J. B. Matson, *ACS Macro Lett.*, 2017, **6**, 1175–1179.
40. J. Liu, A. X. Gao and J. A. Johnson, *JoVE*, 2013, DOI: doi:10.3791/50874, e50874.

41. L. Degennaro, P. Trinchera and R. Luisi, *Chem. Rev.*, 2014, **114**, 7881–7929.
42. Y. Ittah, Y. Sasson, I. Shahak, S. Tsaroom and J. Blum, *J. Org. Chem.*, 1978, **43**, 4271–4273.
43. M. Berry; and D. Craig, *Synlett*, 1992, **1**, 41–44.
44. Z. Ma, Z. Zhou and L. Kürti, *Angew. Chem. Int. Edit.*, 2017, **56**, 9886–9890.
45. B. R. Buckley, A. P. Patel and K. G. U. Wijayantha, *J. Org. Chem.*, 2013, **78**, 1289–1292.
46. C. Bakkali-Hassani, E. Rieger, J. Vignolle, F. R. Wurm, S. Carlotti and D. Taton, *Eur. Polym. J.*, 2017, **95**, 746–755.
47. B. J. Ireland, B. T. Dobigny and D. E. Fogg, *ACS Catal.* , 2015, **5**, 4690–4698.
48. C. Slugovc, S. Demel and F. Stelzer, *Chem. Commun.*, 2002, DOI: 10.1039/B208601H, 2572–2573.
49. N. Kuanr, D. J. Gilmour, H. Gildenast, M. R. Perry and L. L. Schafer, *Macromolecules*, 2022, **55**, 3840–3849.
50. S. E. Blosch, M. Alaboalirat, C. B. Eades, S. J. Scannelli and J. B. Matson, *Macromolecules*, 2022, **55**, 3522–3532.
51. S.-M. Kong, H. Liu, Y.-H. Xue, X.-L. Liu, X.-X. Jia and F.-C. Cui, *Phys. Chem. Chem. Phys.*, 2018, **20**, 24379–24388.
52. N. J. W. Penfold, J. Yeow, C. Boyer and S. P. Armes, *ACS Macro Lett.*, 2019, **8**, 1029–1054.
53. S. Varlas, T. J. Neal and S. P. Armes, *Chem. Sci.* , 2022, **13**, 7295–7303.
54. X. Zhu, Y. Zhou and D. Yan, *J. Polym. Sci. B Polym. Phys.*, 2011, **49**, 1277–1286.
55. X.-M. Liu, T. Lin, J. Huang, X.-T. Hao, K. S. Ong and C. He, *Macromolecules*, 2005, **38**, 4157–4168.
56. A. Mavrič, A. Badasyan, M. Fanetti and M. Valant, *Sci. Rep.*, 2016, **6**, 35450.
57. X. Li, H. ShamsiJazeyi, S. L. Pesek, A. Agrawal, B. Hammouda and R. Verduzco, *Soft Matter*, 2014, **10**, 2008–2015.